

EDINBURGH
INSTRUMENTS



PRECISION RAMAN

Best-in-class Raman microscopes
for research and analytical requirements
backed with world-class customer
support and service.



edinst.com

Raman spectra and structure of hydrogen-bonded water oligomers in tetrahydrofuran–H₂O binary solutions

Ankit Raj¹  | Yu-Jou Chen¹ | Chien-Lung Wang¹  | Hiro-o Hamaguchi^{1,2} 

¹Department of Applied Chemistry and Institute of Molecular Science, National Yang Ming Chiao Tung University, Hsinchu, Taiwan

²Center for Emergent Functional Matter Science, National Yang Ming Chiao Tung University, Hsinchu, Taiwan

Correspondence

Ankit Raj and Hiro-o Hamaguchi, Department of Applied Chemistry and Institute of Molecular Science, National Yang Ming Chiao Tung University, Hsinchu 30010, Taiwan.

Email: ankit@nycu.edu.tw;

hamaguchi@nycu.edu.tw

Funding information

Ministry of Science and Technology, Taiwan, Grant/Award Number: MOST-109-2223-E-009-001-MY3

Abstract

Raman spectra of hydrogen-bonded water oligomers have been resolved from concentration-dependent Raman spectra of tetrahydrofuran (THF)–water binary solutions with the use of multivariate curve resolution with alternating least-squares (MCR-ALS) analysis, assisted by hypothetical addition multivariate analysis with numerical differentiation (HAMAND) procedure. A total of 38 Raman spectra acquired in the broad spectral range of 700–3810 cm⁻¹ were analyzed in a multistep procedure to explain the spectral variations in terms of four components: pure THF, Spectra A, Spectra B, and Spectra C. A four-component MCR-ALS analysis was performed with initial guesses by HAMAND analysis to refine the spectral components and determine their concentration dependence. Of the MCR-ALS resolved three spectra, A was identified as THF(H₂O), B as THF(H₂O)₂ with two hydrogens attached to THF, and C as THF(H₂O)_n having two or more linearly hydrogen-bonded oligomers of water ($n = 2-4$). Observed spectral changes of the OH stretch vibrations of water and those of the C–C/C–O stretches of THF were well reproduced by quantum chemical calculations. Formation of hydrogen-bonded water oligomers in THF–water complexes has thus been revealed. The present study provides a new insight into the basics of hydrogen bonding formation in aqueous systems. It also provides experimental methodology for extracting concentration-dependent minor spectral components contained in complex condensed-phase Raman spectra.

KEYWORDS

hydrogen bonding, molecular complexes, solvent water interaction, THF–water complexes, water oligomers

1 | INTRODUCTION

Water makes a wide variety of hydrogen bonding with itself and with other molecules, playing crucial roles in many molecular systems of physical, chemical, and biological interests. Studies on hydrogen-bonded water oligomers are mandatory for a thorough understanding of the water hydrogen bonding, as well as the bulk

properties of water. Such studies, however, have so far been limited to extremely low temperatures in supersonic-jet expansions or in rare gas matrices. Detection and characterization of hydrogen-bonded water oligomers at ambient temperatures still remains as a challenge. In the present study, we choose the tetrahydrofuran (THF)–water binary system to detect molecular complexes containing hydrogen-bonded water oligomers,

THF:(H₂O)_{*n*} where *n* = 1–4, at room temperature with multivariate curve resolution analysis of concentration-dependent Raman spectra.

The complexes of THF and water have been studied in great detail due to the wide-reaching importance in industry.^[1,2] Formation of cage-like molecular complexes at low temperatures known as clathrates has been discussed extensively.^[2–7] Vibrational spectroscopy is well suited for such studies because the formation and destruction of hydrogen bonds can be well traced with the variation in the molecular vibrational frequencies and intensities specific to water. Mizuno and coworkers studied the hydration of the oxygen atom in THF by observing the concentration dependence of the C–H and C–O stretch vibrations with infrared spectroscopy and ¹J(C–H) with NMR spectroscopy.^[8] They suggested the formation of 1:1 and 1:2 complexes of THF/water up to the concentration of *X*_{H₂O} = 0.9, where *X*_{H₂O} is the molar fraction of water. Schultz and Vu studied the formation of THF–water complexes using infrared spectroscopy at temperature of –5°C.^[5] In their experiments, they used carbon tetrachloride as an infrared inactive medium to observe THF–water complexes formed by mixing 5–25 mM THF in water. On the basis of the wavenumbers and intensities of the two OH stretches, they suggested the formation of the 1:1 and the 1:2 complex. Vallejos and Peruchena performed a detailed theoretical investigation of molecular complexes of the THF with increasing number of water molecules.^[9] They systematically studied a wide variety of possible structures discussing their relative energies and populations. Ojha and coworkers studied the effect of water to the C–O and C–C stretch bands of THF, at various concentrations.^[10] Their work was the primary Raman spectroscopic study on THF–water interactions in the fingerprint region, discussing the features near 900 cm^{–1}. Importantly, they reported the broadening of the strong the C–C stretch band due to the appearance of a shoulder band in the presence of hydrogen-bonded THF. Puryakastha and Madhurima focused on the bulk properties of THF–water binary mixtures, also reporting the infrared spectra,^[11] whereas Sahu and Lee^[12,13] reported early theoretical investigations on the THF–water 1:1 complexes.

In the water-rich domain of THF–water binary system, the structure of complexes has been widely studied because of the formation of clathrates,^[2–7] appearance of anomalous properties,^[14–16] and the particular applications in chemical industry.^[1,2] However, interactions between water and THF are yet unclear in the THF-rich system, where the number of water molecules is too small to form the well-known cage-like structures around the THF molecules. Compared with the water-rich system with abundant hydrogen bonds, the THF-rich system

is a relatively hydrophobic environment with scarce hydrogen bonds. The water molecules are the minor components, and it is reasonable to speculate that complexes composed of single THF molecule with one or more water molecules^[10] will be formed in this hydrophobic environment. Another interesting aspect in the THF-rich system is that the water–water hydrogen bonding may compete with the water–THF hydrogen bonding, due to favorable energetics.^[17,18] In order to understand the actual structures of THF–water complexes in the THF-rich system, the experimental spectral observations are important. With this aim, we investigate the structures of THF–water complexes in the THF-rich system by Raman measurements of binary solutions, focusing on the concentration range of 0.884 to 1 *X*_{THF}, where *X*_{THF} is the molar fraction of THF. After careful calibration of the obtained datasets for relative Raman intensities, laser power fluctuations, and density changes, the spectrum of THF–water complexes were elucidated using the multivariate curve resolution with alternating least-squares (MCR-ALS) assisted by hypothetical addition multivariate analysis with numerical differentiation (HAMAND).

2 | METHODS

2.1 | Materials and sample preparation

Inhibitor-free THF was obtained from Tedia (Tedia Inc., OH, USA) and was used after purification to remove water. A benchtop solvent purification system (LC Technology Solutions Inc., SPBT-1) was used, which utilized low-pressure nitrogen gas to force solvent through various filter materials removing moisture and impurities. Water (resistance 18.2 MΩ) for experiments was obtained by an ultrapure water filtration system (Purity-SP) containing a filter (Millipak 40 Gamma Gold, Millipore, Cat. No. MPGL04GK2, 0.22 μm). THF–water solutions with 38 different concentrations, where a significantly large amount of THF is present relative to water (THF mole fraction, *X*_{THF} ≥ 0.884), were prepared by weighing (XS105 analytical balance with a readability of 0.01 mg, Mettler Toledo). The Raman spectra of these solutions was obtained by measurements using 532-nm laser. Both the sample preparation and Raman measurements were completed within a day.

2.2 | Raman spectroscopic measurements

A laboratory-built confocal Raman microspectrometer with 532.2-nm CW Nd:YVO₄ laser (Verdi-V5, Coherent)

was used. The laser wavelength was monitored and stabilized by a high-resolution wavelength meter (WS-7, HighFinesse) using a DC feedback. The laser power was about 45 mW and was measured continuously during the spectral acquisition using a laser power meter (UP19K-15S-W5 power meter, Gentec-EO) coupled with a high-resolution ADC (PCI-6281 multifunction DAQ, National Instruments). The laser was directed into an inverted microscope (iX71, Olympus) and was focused onto the sample with a long working distance objective lens (SLMPLN 20 \times , NA = 0.25). The fingerprint and high-wavenumber regions of Raman spectra were recorded on two simultaneously controlled CCDs. Scattered light below 580 nm was reflected toward the Acton spectrograph (SP-2500i, Princeton Instruments) equipped with DU970N-BV, CCD (Andor). Scattered light above 580 nm was transmitted through the dichroic filter toward the Kaiser spectrograph (HoloSpec, $f/1.8$) and was detected using DU971N-BV CCD (Andor). With this optical setup, the Raman spectra of liquid samples placed in a quartz cuvette were measured in the fingerprint and high-wavenumber spectral region in conjunction with the laser power in a synchronized manner, utilizing a

computer program developed in LabVIEW.^[19,20] The exposure time for Raman measurements was 15 s each with acquisition of seven spectra per sample. A single quartz cuvette was employed for all measurements. The optical setup is shown in Figure 1.

2.3 | Data analysis

2.3.1 | Spectral correction

Observed spectra were intensity calibrated with the use of the procedure described in our earlier work.^[21,22] In brief, a correction (defined as C_0) for the nonlinear sampling of photons over the wavenumber axis and another correction (defined as C_1) for the relative sensitivity of the Raman spectrometer derived from a tungsten lamp assumed as a broadband blackbody emitter were applied to all the recorded spectra. The power of incident laser was monitored by a laser power meter in tandem with all the Raman measurements. After all experiments, the recorded laser power data were normalized. The spectral intensity of THF–water Raman spectrum was then

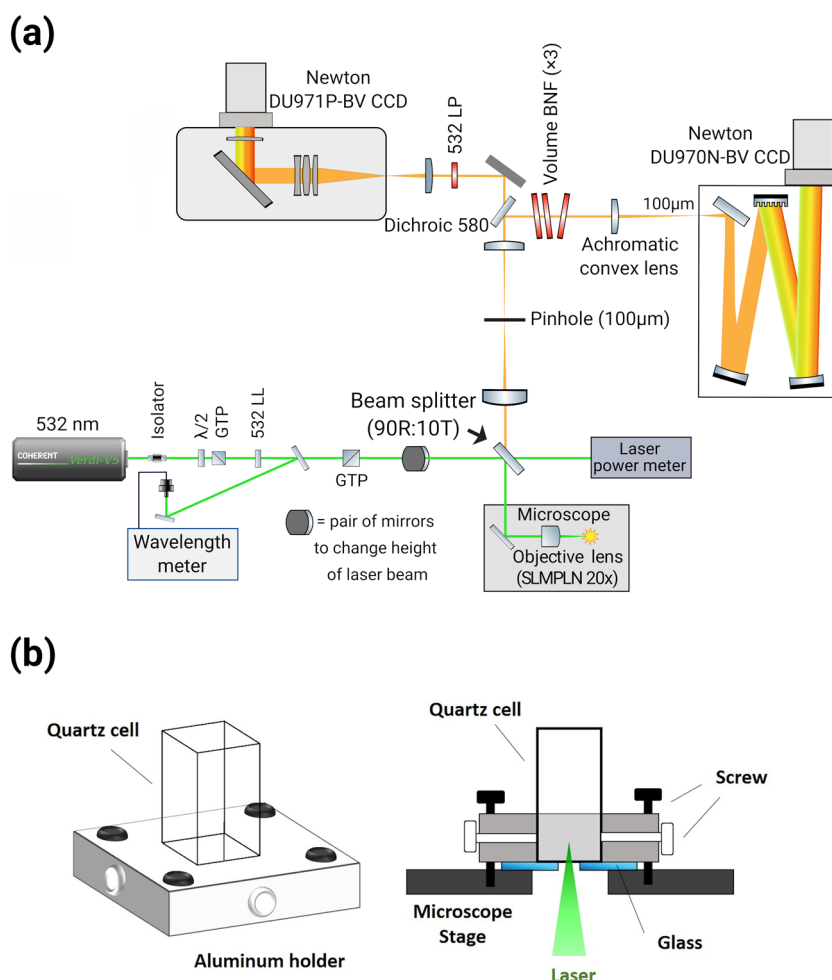


FIGURE 1 (a) The experimental setup of the confocal Raman spectrometer used in the present work. In this Raman spectrometer, a half-wave plate and a Glan–Taylor prism (GTP) are used to attenuate laser power. 532 LL represents laser line filter. Volume BNF represents volume Bragg notch filters. Two CCD detectors are used to measure a broad spectral region spanning from 700 to 3810 cm^{-1} . (b) Sampling setup consisting of a holder fixed to the microscope stage and on which the quartz cuvette containing the sample was reproducibly placed [Colour figure can be viewed at wileyonlinelibrary.com]

divided with the normalized laser power to correct for the laser power variation in each measurement. The maximal laser power variation was found to be around 1.4%. The density of the THF–water mixtures changes with the concentration of the components in the binary mixture. This affects the relative number of molecules present in the confocal volume probed during the Raman measurement. The known densities of THF–water binary mixtures at room temperature were used to determine the required correction for the studied concentrations in our experiments.^[23,24] See Section S1 in the Supporting Information for more details about the corrections to the recorded spectrum.

2.3.2 | Determination of the number of principal spectral components

The number of principal components present in the measured concentration-dependent Raman spectra were estimated by a singular value decomposition^[25] (SVD) analysis of the two-dimensional spectral dataset. The present set of Raman data consists of 38 spectra that correspond to the concentration of THF–water mixture from 0.884 to 1 mol fraction of THF (X_{THF}). The number of different types of THF–water complexes is thought to increase in the system with increasing water molecules. Hence, the SVD analysis was performed on three different sets of Raman spectra, which covered different ranges of concentration: the full set of 38 spectra covering 0.884–1 X_{THF} , the second set of 21 spectra that included 0.933–1 X_{THF} , and lastly a set of 8 spectra that included 0.977–1 X_{THF} .

2.3.3 | MCR-ALS analysis assisted by HAMAND

HAMAND^[26,27] (see Section S2 of the Supporting Information for details) quantitatively determines the contributions of known standard spectra contained in complex overlapping spectra. It facilitates the detection of weak minor spectral components masked by overwhelming spectra from dominant components. According to the precedent SVD analysis, HAMAND was used in three steps to extract the spectra of THF–water complexes (Spectra A, B, and C), which were used as the initial guess spectra for the subsequent MCR-ALS analysis. In the first step, observed spectrum at $X_{\text{THF}} = 0.977$ was analyzed by HAMAND to separate the spectrum of pure THF and Spectrum A, where pure THF spectrum was used as the known standard and Spectrum A was obtained as HAMAND subtraction residual. In the

second step at $X_{\text{THF}} = 0.933$, pure THF spectrum and Spectrum A obtained in the first step were used as the standard to extract Spectrum B as the HAMAND subtraction residual. In the third step at $X_{\text{THF}} = 0.884$, pure THF spectrum and two complex Spectra A and B were used as standard to obtain spectrum C. A four-component MCR-ALS analysis^[28] (see Section S2 of the Supporting Information) was then carried out with the use of HAMAND extracted spectra as initial guess spectra to refine Spectra A, B, and C and simultaneously determine their concentration dependence.

3 | RESULTS

3.1 | Concentration-dependent Raman spectra of THF–water solutions

Raman spectra of THF–water binary mixtures, after intensity calibration procedure, are shown in Figure 2. These spectra correspond to the binary mixture where a large amount of THF is present relative to water. In these spectra, the strong Raman peak at about 910 cm^{-1} is the most prominent feature, which is composed of a strong C–C stretch at 914 cm^{-1} and a much weaker C–O stretch at around 910 cm^{-1} . These vibrations of THF are sensitive to the formation of hydrogen bonds with water.^[10] The inset shows the OH stretch vibrations from THF–water complexes observed in the present experiments. Unlike the broad feature of the OH stretch bands observed in bulk water, here, two well-defined Lorentzian peaks are noticed whose spectral parameters (intensity and bandwidth) changes with increasing water concentration.

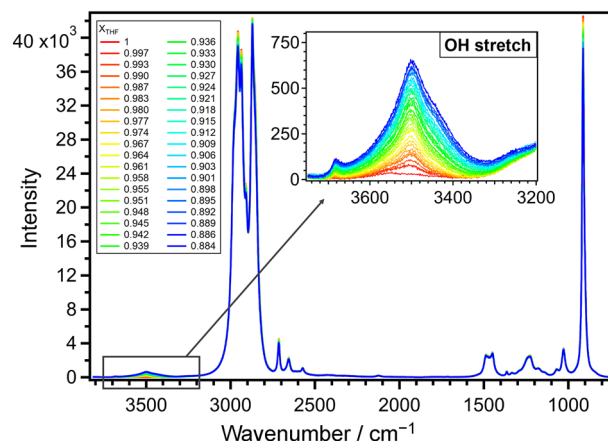


FIGURE 2 Raman spectra of water–THF solutions at different concentrations (X_{THF}). The inset shows the zoom-in view of the OH stretch region [Colour figure can be viewed at wileyonlinelibrary.com]

3.2 | Determination of the number of principal spectral components by SVD analysis

The number of different types of THF–water complexes is expected to increase in the system with increasing water molar fraction. Hence, as described in Section 2.3, SVD analyses were performed on three different set of Raman spectra covering different ranges of concentrations. The results of this analysis are summarized in Figure 3. In the concentration range $0.977 \leq X_{\text{THF}} \leq 1$, the SVD singular values are shown in blue color, where the two relatively large singular values indicate that the spectral changes in this concentration range are due to two distinct components. In the concentration range $0.933 \leq X_{\text{THF}} \leq 1$, SVD singular values are displayed in green color, where values of the third and the fourth SVD component rise, in comparison with the blue points. This fact indicates that, in total, there are four components dominating the spectral changes, with the fraction of fourth component being the lowest. Lastly, in the full concentration range $0.884 \leq X_{\text{THF}} \leq 1$, the orange singular values clearly show that there are four components

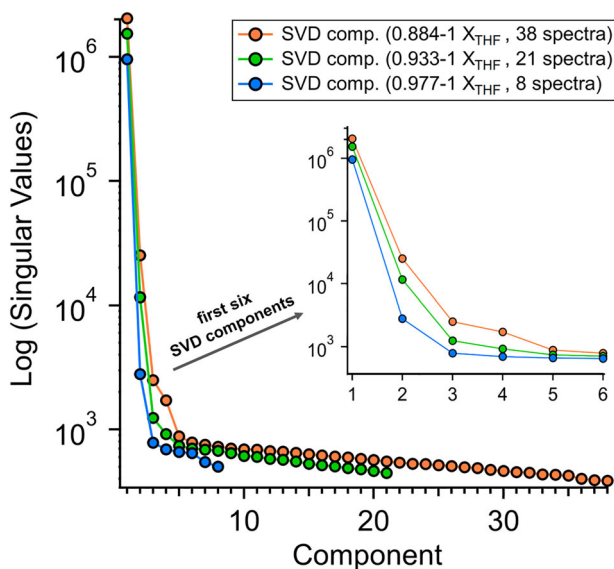


FIGURE 3 Singular values derived from SVD analysis of the concentration-dependent Raman spectra of the THF–water solutions. The inset is the zoom-in view for the first six SVD components. The blue, green, and orange points of the SVD components correspond to analysis of three different sets of concentration-dependent Raman spectra. The SVD singular values on analyzing (i) eight spectra in the concentration range of $0.977-1 X_{\text{THF}}$ are shown in blue, (ii) 21 spectra in the concentration range of $0.933-1 X_{\text{THF}}$ are shown in green, and (iii) 38 spectra in the concentration range of $0.884-1 X_{\text{THF}}$ are shown in orange, respectively [Colour figure can be viewed at wileyonlinelibrary.com]

dominating the spectral variation. These results of SVD analysis provide an estimate of the number of principal components existing in the THF–water solutions in the studied concentration range and three minor spectral components, Spectra A, B, and C, which are thought to be from THF–water complexes.

3.3 | Initial guess spectra for MCR-ALS analysis obtained by HAMAND analysis

MCR-ALS analysis often requires one or more first guess spectra to reach a correct and physically meaningful convergence of the least-squares optimization procedure. The correctness of obtained final results relies to a large degree on the quality of the initial guess. In the present study, we effectively utilize the initial guesses determined by HAMAND. According to the earlier SVD analysis, the $0.977 X_{\text{THF}}$ solution consists of two components (pure THF and Spectrum A). HAMAND analysis with the Raman spectra of pure THF as the standard gives Spectrum A as shown in Figure 4a. The Raman spectrum at $X_{\text{THF}} = 0.933$ is then assumed to consist of three major components (pure THF, Spectrum A, and Spectrum B) with the fourth component considered to be negligible. In order to obtain Spectrum B, the pure THF Raman signal is subtracted first by HAMAND. The resulting spectrum corresponded to a linear combination of Spectrum A and Spectrum B. Again, HAMAND subtracts Spectrum A (obtained from previous analysis) to give Spectrum B, as shown in Figure 4b. Similarly, the Raman spectrum at $X_{\text{THF}} = 0.884$ consists of four components (pure THF, Spectrum A, Spectrum B, and Spectrum C). The spectra of pure THF and Spectra A and B are sequentially subtracted by HAMAND to obtain Spectrum C shown in the Figure 4c.

Overall, we obtain four spectral components, namely, pure THF, Spectrum A, Spectrum B, and Spectrum C, as shown in Figure 5. Here, we make an assumption that the spectrum at $X_{\text{THF}} = 0.933$ consists of only three components although the fourth component may already exist in a small amount. Therefore, Spectra B and C are refined and finalized by the subsequent MCR-ALS analysis.

3.4 | Four-component MCR-ALS analysis of the concentration-dependent Raman spectra

A total of 38 Raman spectra spanning the concentration from 0.884 to $1 X_{\text{THF}}$ were used as the input matrix. The number of spectral components were determined to be

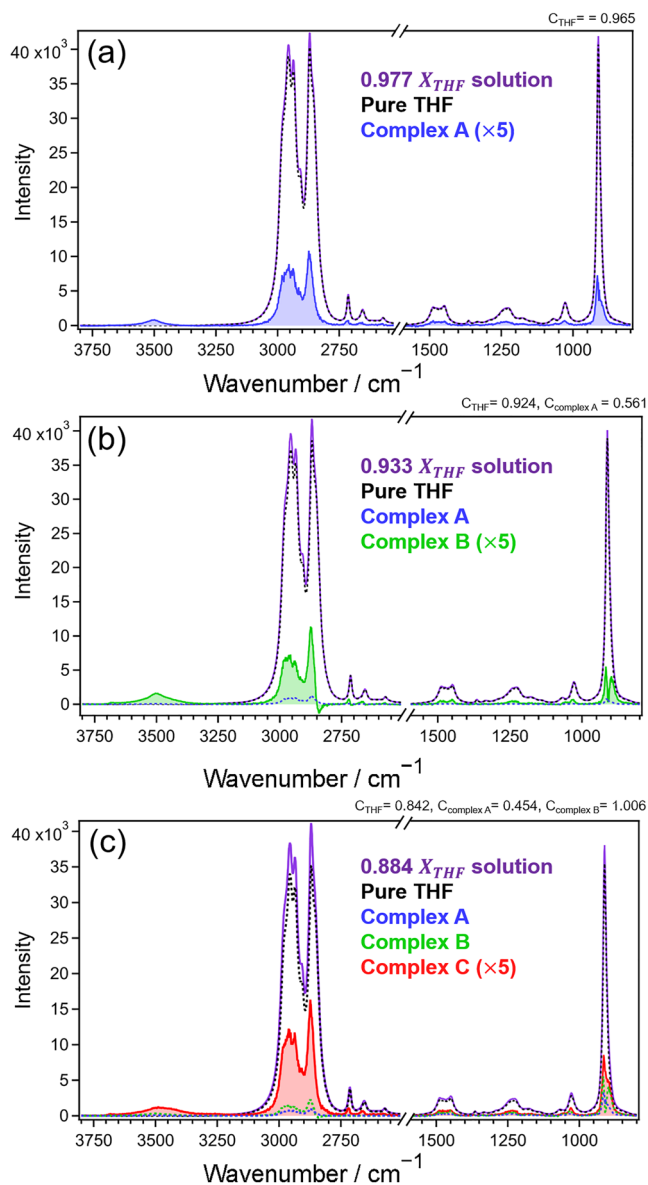


FIGURE 4 The results of HAMAND analysis. Raman spectrum of the known components (dashed line) subtracted from the spectra of solutions (solid purple), obtaining the spectra of unknown components (filled line). (a) Raman spectrum for the $0.977 X_{THF}$ solution (solid purple), pure THF (dashed black), and the resulting spectrum of Complex A (filled red) that is enlarged by five times. (b) Raman spectrum for the $0.933 X_{THF}$ solution (solid purple), pure THF (dashed black), complex A (dashed blue), and the resulting spectrum of Complex B (filled green) that is enlarged by five times. (c) Raman spectrum for the $0.884 X_{THF}$ solution (solid purple), pure THF (dashed black), Complex A (dashed blue), Complex B (dashed green), and the resulting spectrum of Complex C (filled red) that is enlarged by five times [Colour figure can be viewed at wileyonlinelibrary.com]

four from the SVD analysis described earlier. For the initial guess spectra, the four spectra (pure THF, Spectrum A, Spectrum B, and Spectrum C) obtained from

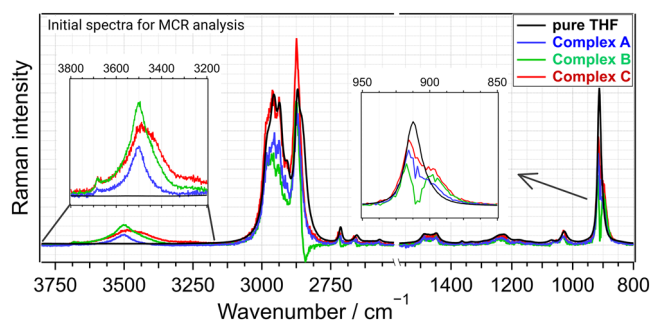


FIGURE 5 The four initial spectra used for the MCR-ALS analysis obtained by a preceding HAMAND analysis. The inset shows the zoom-in view in the OH stretch region and THF ring breath region [Colour figure can be viewed at wileyonlinelibrary.com]

HAMAND analysis were used. During this optimization process, the spectra of pure THF and Spectrum A were fixed, whereas the other two components were free to change. The results thus obtained are shown in Figure 6. The spectral information shows that the MCR-ALS resolved spectra are almost identical to the initial guess spectra from HAMAND with only a few small changes. It is noteworthy that the negative feature at about 2770 cm^{-1} in the green spectrum (Figure 5), which is physically wrong, disappears after MCR-ALS refinement, indicating that the accuracy of the spectral analysis is improved. Figure 6a shows the Raman spectrum of pure THF (black) and the other three spectra: Spectrum A (blue), Spectrum B (green), and Spectrum C (red).

MCR-ALS analysis also provides the concentration-dependent fractions of the four components as shown in Figure 6b. The fraction of pure THF (black) linearly decreases with increasing water concentration. The fraction of Spectrum A (blue) increases rapidly with increasing water concentration above $X_{THF} = 0.975$ and makes a plateau for $X_{THF} < 0.975$. With water concentration continuously increasing, Spectrum A gradually gets replaced by Spectra B and C to make the fractions of B and C increase for when $X_{THF} < 0.977$. This result is consistent with the SVD analysis, which indicates that the solution is a two-component system in the concentration of $X_{THF} > 0.977$ and four-component system for $X_{THF} < 0.977$.

4 | DISCUSSION

4.1 | Assignments of the three MCR-ALS resolved spectra

Three spectra—Spectrum A, Spectrum B and Spectrum C—have been resolved with MCR-ALS (see Figure 6).

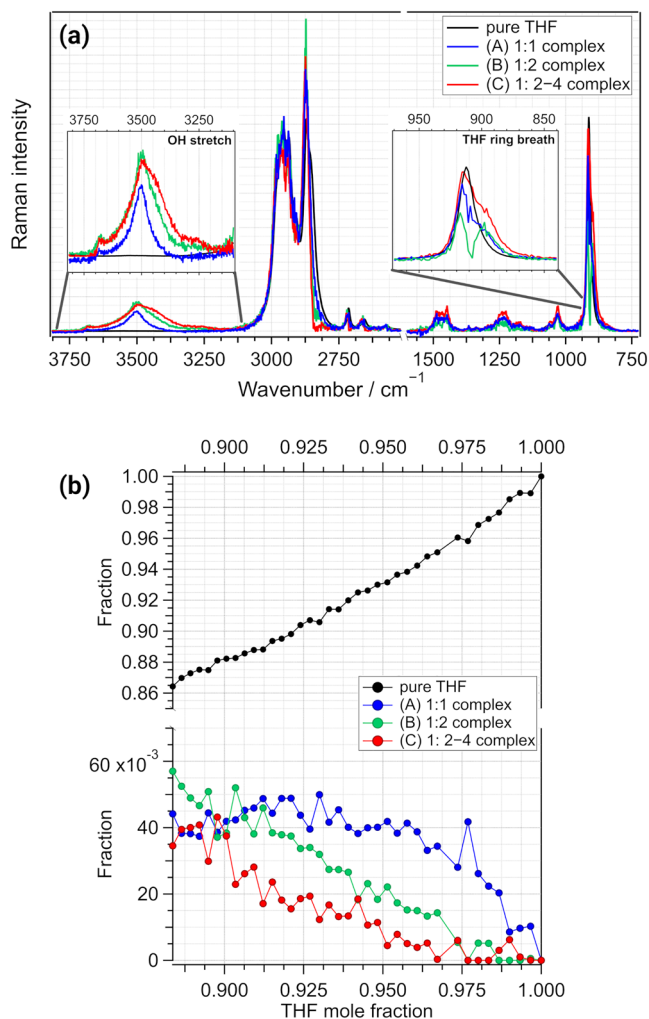


FIGURE 6 The results of MCR-ALS analyzed with four components. (a) Raman spectra of four components, pure THF (black line), 1:1 complex (blue line), 1:2 complex (green line), and 1: n ($n = 2 - 4$) complex (red line). The inset is the zoom-in view in the THF ring breath and OH stretch region. (b) Concentration-dependent fractions of pure THF (black line) and the three THF-water complexes [Colour figure can be viewed at wileyonlinelibrary.com]

We now assign these three spectra to THF-water complexes. Spectrum A is straightforwardly assigned to the 1:1 complex of THF with water. It shows two symmetric Lorentzian band centered at 3687 and 3504 cm^{-1} in the OH stretch region. The Lorentzian band shapes means that the two bands are homogeneously broadened and that they originate from single isolated water molecule in the 1:1 complex. The 3687 cm^{-1} band is characteristic of the OH stretch vibration, which is free of any hydrogen bonding interaction, as supported by similar observations of monomeric water in deuterium matrix by Murby and Pullin,^[29] and high-resolution

Raman spectra and theoretical investigations of water vapor by Avila and coworkers.^[30,31] Such 1:1 complex of THF with water was also noted by Shultz and Vu^[5] using infrared spectroscopy, who reported the band at 3685 cm^{-1} , which agrees within experimental uncertainty with the present observation. In the $850\text{--}950\text{ cm}^{-1}$ region, the convolution of THF CC/CO stretch bands of the 1:1 complex is broader than that of the pure THF molecule, showing that THF interacts with water molecules and the ring CC/CO stretch modes are affected by this interaction.

Spectrum B in Figure 6 shows two OH stretching bands, similar in position as observed in Spectrum A. However, the OH stretch band at 3504 cm^{-1} is broadened toward the lower wavenumber side, relative to Spectrum A, suggesting the presence of an extra water molecule in the complex. In the fingerprint region ($850\text{--}950\text{ cm}^{-1}$), the THF CC/CO stretch band splits into two peaks. This splitting indicates that the THF molecule is more profoundly affected by water molecules. See Section 4.2 for further details. Spectrum C shows two extra bands, a shoulder around 3450 cm^{-1} and a broad peak around 3250 cm^{-1} in addition to the two bands existing in Spectra A and B. These extra bands must come from further extra water molecules contained in the complex. The THF CC/CO stretch band of Spectrum C is close to that of Spectrum A, suggesting that THF interacts with water in a similar way as in the 1:1 complex (Spectrum A).

The 3687 cm^{-1} OH stretch band, which is characteristic of the non-hydrogen-bonded dangling OH, is also visible in Spectra B and C (Figure 2 and in Figure 6a). By comparing the peak area of this dangling OH band with that of Spectrum A (1:1 complex), the number of water molecules in Spectra B and C can be quantified. To do this, the spectra obtained from MCR-ALS analysis were first normalized to the band area of the CH stretch signal of THF. Next, in order to analyze the peak area of the dangling OH band, as well as to minutely analyze other features, Lorentzian functions were used to fit the observed OH stretch bands. The results are shown in the Figure 7. The peak areas of the dangling OH bands in the three spectra are found in the ratio of 1:2:3.14 for A:B:C. The ratio 1:2 for A:B indicates that Spectrum B is contributed by two dangling OH bonds. Considering the fact that THF is more profoundly affected by hydrogen bonding (splitting of the CC/CO stretch mode), we assign Spectrum B to the bidentate 1:2 THF-water complex in which two water molecules are attached to THF (Figure 8a). The ratio 3.14 (not an integer) indicates that Spectrum C is contributed by plural number of different THF-water complexes. THF-water complexes with 2, 3, and 4 water molecules linearly hydrogen bonded

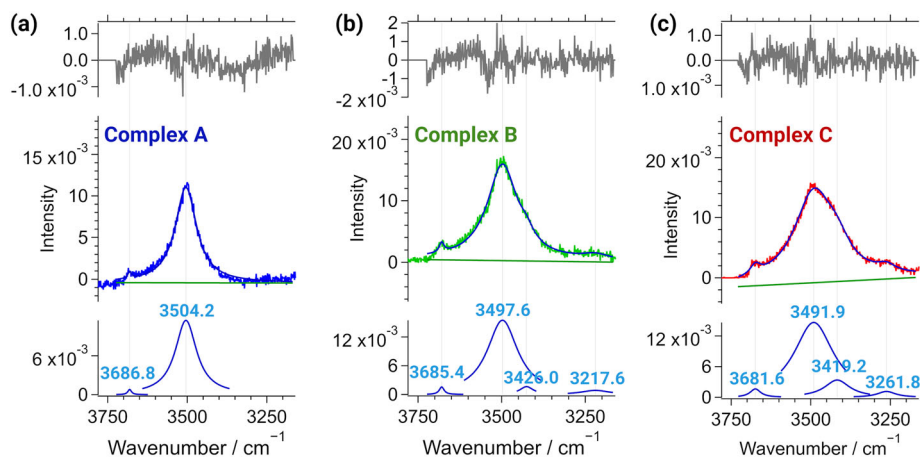


FIGURE 7 Results on the curve fitting of Raman spectra of THF–water complexes in OH stretch region. The fit functions and the residuals are shown in blue color and gray colors, respectively. (a) The Raman spectrum of the 1:1 THF–water complex fitted with two Lorentzian bands. (b) The Raman spectrum of 1:2 complex fitted with four Lorentzian bands. (c) The Raman spectrum of 1:2–4 complex fitted with four Lorentzian bands [Colour figure can be viewed at wileyonlinelibrary.com]

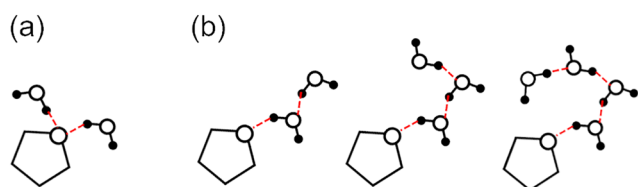


FIGURE 8 The possible models of Complex B (1:1 THF–water complex) and C (1: 2–4 THF water complex). (a) Complex B is the 1:2 complex composed of one THF attached to two water molecules, forming two water–THF hydrogen bonds. (b) The structure of complex C is likely a dynamic mixture of 1:2, 1:3, and 1:4 complexes featuring both water–water and THF–water hydrogen bonding [Colour figure can be viewed at wileyonlinelibrary.com]

(Figure 8b), are the most likely contributors to Spectrum C. Note that the number of dangling OH bond is 2, 3, and 4 for the three water oligomers contained in the 1:2, 1:3, and 1:4 complexes. Dynamic or static mixture of the three complexes may well give the ratio 3.14. The similarity of the THF CC/CO stretch band in Spectrum C to that of Spectrum A (1:1 complex) also supports the structures shown in Figure 8b in which only one water–THF hydrogen bond is formed.

To sum up, Spectrum A is assigned to the 1:1 THF–water complex, Spectrum B to the bidentate 1:2 complex with two water molecule attached to THF, and Spectrum C to a mixture of 1:2, 1:3, and 1:4 complexes where water molecules form linear chain hydrogen bonding. Every added water forms the hydrogen bond with THF for $X_{THF} > 0.977$ to form the 1:1 complex. If more water is continuously added, new complexes, 1:2, 1:3, and 1:4 complexes, start to appear, whereas the fraction of the 1:1 complex makes a plateau (see Figure 6b). Two different types of 1:2 complexes,

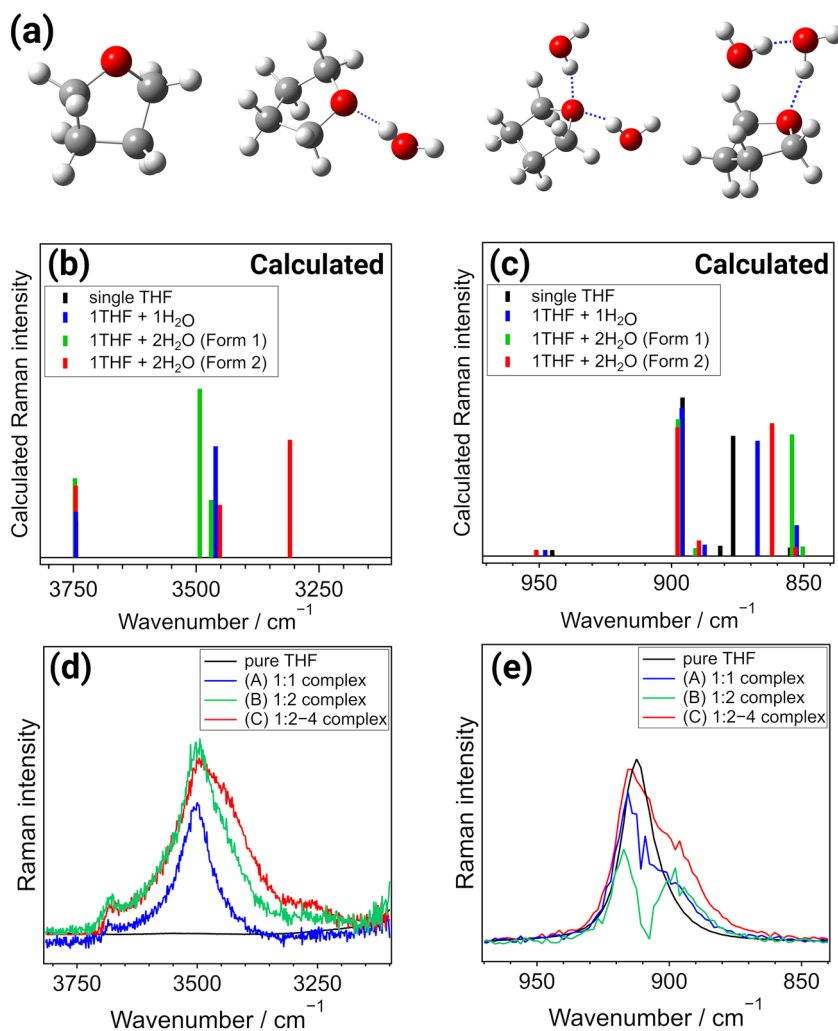
bidentate 1:2 complex with two water molecules hydrogen-bonded to THF (Spectrum B), and linear 1:2 complex in which two water molecules makes a chain with one hydrogen bonding with THF (one component in Spectrum C) have been identified. Both dynamic and static mixtures are possible for the three complexes to make Spectrum C.

4.2 | Insights from quantum chemical calculations

Quantum chemical calculations were performed to theoretically confirm the assignments of MCR-ALS resolved three Raman spectra A, B, and C of THF–water complexes. All calculations were performed using Gaussian 16 package (Gaussian 16, Revision A.03).^[32] The optimized geometries and Raman spectra of the THF molecule and THF–water complexes were calculated with the use of DFT method utilizing aug-cc-pVTZ basis set. B3LYP was chosen as density functional for these calculations. Dispersion correction, namely GD3,^[33] was included for the functional, and anharmonic correction^[34–36] to the vibrational wavenumbers were applied. Refer to Section S4 of the Supporting Information for further details on the calculations.

Figure 9a shows the optimized geometries of the THF molecule and three THF–water molecular complexes: the 1:1 complex and two forms of the 1:2 complex (bidentate and linear). The corresponding calculated Raman spectra in the OH stretch and THF CC/CO stretch regions are shown in Figure 9b,c using colored sticks. Zoomed-up parts of the experimental results are shown in Figure 9d,e. The calculated Raman spectra are displayed as black sticks for THF, blue for the 1:1 complex, green for the bidentate 1:2 complex, and red for the linear 1:2 complexes.

FIGURE 9 The results of quantum chemical calculations. (a) Optimized geometries of single THF, the complex of THF with one H₂O, and the THF with two H₂O (Form 1 and Form 2). The calculated Raman spectra of single THF, the complex of THF with one H₂O, and the THF with two H₂O in (b) the OH stretch region and (c) the THF ring breath region. The measured Raman spectra of pure THF, 1:1 complex (A), 1:2 complex (B) and 1:2–4 complex (C) from the MCR-ALS analysis in (d) the OH stretch region and (e) the THF ring breath region [Colour figure can be viewed at wileyonlinelibrary.com]



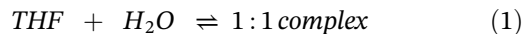
Two distinct OH stretch bands, dangling OH and hydrogen-bonded OH, are calculated for the 1:1 complex (blue) showing good agreement with the experimental spectrum (Figure 9d, blue). For the bidentate 1:2 complex (green) and linear 1:2 complex (red), two extra OH stretch bands are calculated in the lower wavenumber side in addition to the two bands in the 1:1 complex. This result again is consistent with the experimental spectra in which extra OH stretch bands appear in the lower wavenumber side of the OH stretch region (Figure 9d, green and red). In the fingerprint region between 800 and 950 cm⁻¹, two prominent CC/CO stretch bands of THF are calculated. CO stretch at around 878 cm⁻¹ and CC stretch at 896 cm⁻¹. The splitting between these two is the smallest for THF (black stick) and the largest for the bidentate 1:2 complex (green). For the 1:1 complex (blue) and linear 1:2 complex (red), the magnitude of the splitting is in between as that observed for single THF and the bidentate 1:2 complex. This calculation results well explain the experimental observation that

only one (overlapping of two CC/CO stretches) band is observed for THF, split two bands for the bidentate 1:2 complex, and asymmetric bands with shoulders in the low wavenumber side for the 1:1 complex and the linear 1:2 complex. This observation in the fingerprint region is also found to be in agreement with the Raman measurements of Ojha and coworkers.^[10] The calculations thus fully support the assignments of the MCR-ALS resolved three spectra A, B, and C to the 1:1 complex, bidentate 1:2 complex, and linear 1:*n* complex (*n* = 2–4).

4.3 | Equilibrium constant for the formation of the 1:1 complex

The fractions of molecular complexes along with free THF molecule must result from thermal equilibrium at a given concentration of the binary mixture. The equilibrium constant for the formation of the 1:1 complex in the two-component system ($X_{THF} > 0.977$) is obtained by

using the fraction of the 1:1 complex determined from the MCR-ALS analysis. At a constant temperature (298.15 K), and assuming an equilibrium between the free THF and free water, the reversible reaction is expressed as



Equilibrium constant for this reaction ($K_{eq,1}$) is then defined as

$$K_{eq,1} = \frac{x}{(X_{THF} - x)(1 - X_{THF} - x)}, \quad (2)$$

where x is the fraction of the 1:1 complex. Rearranging Equation 2 gives

$$K_{eq,1}x^2 + (-K_{eq,1} - 1)x + (-X_{THF}^2 + X_{THF})K_{eq,1} = 0 \quad (3)$$

Assuming certain value of $K_{eq,1}$ the solution of Equation 3 for x is found. Of the two possible solutions of the quadratic equation (Equation 3), the correct solution is selected by choosing value of x , which is reasonable (i.e., a real number lower than 1 and X_{THF} in magnitude).

In order to utilize the MCR-ALS determined molecular fractions to determine the value of $K_{eq,1}$, we use the following procedure. Nonlinear least squares^[22,37] fitting is applied to the MCR-ALS determined concentration-dependent fractions of THF and water. First, the solution for the fraction of 1:1 complex x for all available concentrations is computed as a vector, \vec{x} . The remaining THF in the two-component system is then computed as $\vec{T} = (1 - \vec{x})$. The results from the MCR-ALS analysis for the fraction of 1:1 complex (\vec{x}^{MCR}) and THF (\vec{T}^{MCR}) are compared with corresponding calculated results \vec{x} and $\vec{T} = (1 - \vec{x})$.

$$\Delta \vec{x} = \vec{x} - \vec{x}^{MCR} \quad (4)$$

$$\Delta \vec{T} = \vec{T} - \vec{T}^{MCR} = (1 - \vec{x}) - \vec{T}^{MCR} \quad (5)$$

Sum of squares of the differences are used to form a measure of difference between the computed and experimental data expressed below as E .

$$E = \left| \Delta \vec{x} \right|^2 + \left| \Delta \vec{T} \right|^2 \quad (6)$$

$$\min(E) : K_{eq,1}$$

Lastly, an iterative minimization of E using the MCR results gives an appropriate value of $K_{eq,1}$. The so computed value of $K_{eq,1}$ was 10,400, indicating that all the water molecules added to the system in the concentration range $X_{THF} > 0.977$ form the 1:1 complex.

4.4 | General discussion

The THF–water complexation structures determine the solvent property of the water–THF mixtures. Although the water structure in the water-rich domain is well understood, there remains limited studies investigating the molecular complexes in the THF-rich domain. The present study proves the formation of three different THF–water complexes: 1:1, bidentate 1:2, and linear 1: n ($n=2-4$) complexes. Water molecules have a tendency to actively form hydrogen bonds among themselves rather than with free THF. The water structure in the THF-rich region is thus shown very different from that of the water-rich region, where hydrogen-bonded water cage structures are well known. The detection of the dangling OH band at $\sim 3690 \text{ cm}^{-1}$ is characteristic of the water structures in the THF-rich region of the binary mixture.

The Raman spectrum of the 1: n ($n=1-4$) complex is worth special mention. It much resembles the Raman spectrum of destructured hydrogen-bonded water extracted from the temperature-dependent Raman spectra of liquid water^[38] with a peak at around 3500 cm^{-1} and a shoulder at low wavenumber side. It is highly likely that linearly hydrogen-bonded dimer, trimer, tetramers, and larger complexes are the main constituents of destructured hydrogen-bonded water in the condensed phase.

5 | CONCLUSION

A carefully calibrated set of concentration-dependent Raman spectra of THF–water binary solutions have been analyzed with MCR-ALS analysis assisted by HAMAND. The analysis proves the formation of three different THF–water complexes: the 1:1 complex, the bidentate 1:2 complex, and the linear 1: n ($n=2-4$) complex. The water hydrogen bonding scheme elucidated in the present study for the THF-rich region sharply contrasts to the known hydrogen-bonded cage structures in the water-rich domain. The spectrum of the 1:1 complex shows two homogeneously broadened OH stretch bands characteristic of isolated single water molecules. The spectrum of the linear 1: n complex resembles the previously reported spectrum of destructured

hydrogen-bonded water, thus giving a clue to understand more deeply the structure of ambient liquid water. In addition, the present study has demonstrated a general experimental approach to extract spectra at a single molecular level in the condensed phase.

ACKNOWLEDGEMENTS


The present work formed the master thesis of YJC, National Yang Ming Chiao Tung University, July 2021. This research was funded by Ministry of Science and Technology, Taiwan with project MOST-109-2223-E-009-001-MY3.


DATA AVAILABILITY STATEMENT

Additional information supporting the findings of this study is openly available via the supplementary material document. Programs used in the data analysis process are available in the online repository at GitHub accessible via <https://doi.org/10.5281/zenodo.4926168>, reference number 22.

ORCID

Ankit Raj  <https://orcid.org/0000-0002-2495-3354>

Chien-Lung Wang  <https://orcid.org/0000-0002-4799-4730>

Hiro-o Hamaguchi  <https://orcid.org/0000-0002-4320-0921>

REFERENCES

- [1] H. Zeng, L. D. Wilson, V. K. Walker, J. A. Ripmeester, *J. Am. Chem. Soc.* **2006**, *128*(9), 2844.
- [2] H. Lee, J.-w. Lee, D. Y. Kim, J. Park, Y.-T. Seo, H. Zeng, I. L. Moudrakovski, C. I. Ratcliffe, J. A. Ripmeester, *Materials For Sustainable Energy: A Collection of Peer-Reviewed Research and Review Articles from Nature Publishing Group*, World Scientific, UK **2011** 285.
- [3] H. Conrad, F. Lehmkuhler, C. Sternemann, A. Sakko, D. Paschek, L. Simonelli, S. Huotari, O. Feroughi, M. Tolan, K. Hämmäläinen, *Phys. Rev. Lett.* **2009**, *103*(21), 218301.
- [4] M. Kato, S. Matsumoto, A. Takashima, Y. Fujii, Y. Takasu, I. Nishio, *Vib. Spectrosc.* **2016**, *85*, 11.
- [5] M. J. Shultz, T. H. Vu, *J. Phys. Chem. B.* **2015**, *119*(29), 9167.
- [6] T. Yagasaki, M. Matsumoto, H. Tanaka, *J. Phys. Chem. C* **2016**, *120*(6), 3305.
- [7] T. M. Vlastic, P. D. Servio, A. D. Rey, *Ind. Eng. Chem. Res.* **2019**, *58*(36), 16588.
- [8] K. Mizuno, Y. Masuda, T. Yamamura, J. Kitamura, H. Ogata, I. Bako, Y. Tamai, T. Yagasaki, *J. Phys. Chem. B.* **2009**, *113*(4), 906.
- [9] M. M. Vallejos, N. M. Peruchena, *J. Phys. Chem. A* **2012**, *116*(16), 4199.
- [10] A. K. Ojha, S. K. Srivastava, N. Peica, S. Schlücker, W. Kiefer, B. Asthana, *J. Mol. Struct.* **2005**, *735*, 349.
- [11] D. D. Purkayastha, V. Madhurima, *J. Mol. Liq.* **2013**, *187*, 54.
- [12] P. K. Sahu, A. Chaudhari, S. L. Lee, *Chem. Phys. Lett.* **2004**, *386*(4–6), 351.
- [13] P. K. Sahu, S. L. Lee, *J. Chem. Phys.* **2005**, *123*(4), 044308.
- [14] F. M. Winnik, H. Ringsdorf, J. Venzmer, *Macromolecules* **1990**, *23*(8), 2415.
- [15] F. M. Winnik, M. F. Ottaviani, S. H. Bossmann, W. Pan, M. Garcia-Garibay, N. J. Turro, *Macromolecules* **1993**, *26*(17), 4577.
- [16] J. Hao, H. Cheng, P. Butler, L. Zhang, C. C. Han, *J. Chem. Phys.* **2010**, *132*(15), 154902.
- [17] I. A. Sedov, B. N. Solomonov, *J. Phys. Org. Chem.* **2012**, *25*(12), 1144.
- [18] L. Gomide Freitas, J. Marques Cordeiro, *J. Mol. Struct.: THEOCHEM* **1995**, *335*, 189.
- [19] C. Elliott, V. Vijayakumar, W. Zink, R. Hansen, *J. Assoc. Lab. Autom.* **2007**, *12*(1), 17.
- [20] C. J. Kalkman, *J. Clin. Monit. Comput.* **1995**, *11*(1), 51.
- [21] A. Raj, C. Kato, H. A. Witek, H. O. Hamaguchi, *J. Raman Spectrosc.* **2020**, *51*(10), 2066.
- [22] A. Raj, RamanSpec_BasicOperations: Igor procedures for Raman data analysis. **2021**. https://github.com/ankit7540/RamanSpec_BasicOperations
- [23] A. Schedemann, E. C. Ihmels, J. Gmehling, *Fluid Phase Equilib.* **2010**, *295*(2), 201.
- [24] O. Kiyohara, P. J. D'Arcy, G. C. Benson, *Can. J. Chem.* **1978**, *56*(22), 2803.
- [25] G. H. Golub, C. F. V. Loan, *Matrix Computations*, 3rd ed., Johns Hopkins University Press, Baltimore, MD **1996**.
- [26] M. Ando, I. K. Lednev, H. Hamaguchi, *Frontiers and Advances in Molecular Spectroscopy*, Elsevier, Amsterdam, Netherlands **2018** 369.
- [27] M. Ando, H. Hamaguchi, *J. Spectros. Soc. Jpn* **2015**, *64*(1), 280.
- [28] M. Ando, H. Hamaguchi, *J. Biomed. Opt.* **2014**, *19*(1), 011016.
- [29] E. Murby, A. Pullin, *Aust. J. Chem.* **1979**, *32*(6), 1167.
- [30] G. Avila, G. Tejada, J. M. Fernandez, S. Montero, *J. Mol. Spectrosc.* **2004**, *223*(2), 166.
- [31] G. Avila, J. M. Fernandez, G. Tejada, S. Montero, *J. Mol. Spectrosc.* **2004**, *228*(1), 38.
- [32] M. J. Frisch, G. W. Trucks, H. B. Schlegel, G. E. Scuseria, M. A. Robb, J. R. Cheeseman, G. Scalmani, V. Barone, G. A. Petersson, H. Nakatsuji, X. Li, M. Caricato, A. V. Marenich, J. Bloino, B. G. Janesko, R. Gomperts, B. Mennucci, H. P. Hratchian, J. V. Ortiz, A. F. Izmaylov, J. L. Sonnenberg, D. Williams, F. Ding, F. Lipparini, F. Egidi, J. Goings, B. Peng, A. Petrone, T. Henderson, D. Ranasinghe, V. G. Zakrzewski, J. Gao, N. Rega, G. Zheng, W. Liang, M. Hada, M. Ehara, K. Toyota, R. Fukuda, J. Hasegawa, M. Ishida, T. Nakajima, Y. Honda, O. Kitao, H. Nakai, T. Vreven, K. Throssell, J. A. Montgomery Jr., J. E. Peralta, F. Ogliaro, M. J. Bearpark, J. J. Heyd, E. N. Brothers, K. N. Kudin, V. N. Staroverov, T. A. Keith, R. Kobayashi, J. Normand, K. Raghavachari, A. P. Rendell, J. C. Burant, S. S. Iyengar, J. Tomasi, M. Cossi, J. M. Millam, M. Klene, C. Adamo, R. Cammi, J. W. Ochterski, R. L. Martin, K. Morokuma, O. Farkas, J. B. Foresman and D. J. Fox, Wallingford, CT, **2016**.
- [33] S. Grimme, J. Antony, S. Ehrlich, H. Krieg, *J. Chem. Phys.* **2010**, *132*(15), 154104.

- [34] S. Califano, *Vibrational States*, Wiley, London; New York **1976**.
- [35] W. H. Miller, N. C. Handy, J. E. Adams, *J. Chem. Phys.* **1980**, 72(1), 99.
- [36] D. A. Clabo, W. D. Allen, R. B. Remington, Y. Yamaguchi, H. F. Schaefer, *Chem. Phys.* **1988**, 123(2), 187.
- [37] W. H. Press, S. A. Teukolsky, W. T. Vetterling, B. P. Flannery, *Numerical Recipes in C: The Art of Scientific Computing*, 2nd ed., Cambridge University Press, New York, USA **1992**.
- [38] H. Okajima, M. Ando, H. Hamaguchi, *B Chem. Soc. Jpn* **2018**, 91(6), 991.

SUPPORTING INFORMATION

Additional supporting information may be found in the online version of the article at the publisher's website.

How to cite this article: A. Raj, Y.-J. Chen, C.-L. Wang, H. Hamaguchi, *J Raman Spectrosc* **2022**, 1.
<https://doi.org/10.1002/jrs.6381>